Geofísica Internacional
ISSN: 0016-7169
silvia@geofisica.unam.mx
Universidad Nacional Autónoma de México
México

Coconi-Morales, E.; Ronquillo-Jarillo, G.; Campos-Enríquez, J. O.
Multi-scale analysis of well-logging data in petrophysical and stratigraphic correlation
Geofísica Internacional, vol. 49, núm. 2, abril-junio, 2010, pp. 55-67
Universidad Nacional Autónoma de México
Distrito Federal, México

Geofísica Internacional 49 (2), 55-67 (2010)

Multi-scale analysis of well-logging data in petrophysical and stratigraphic correlation

E. Coconi-Morales[1*], G. Ronquillo-Jarillo[1], J. O. Campos-Enríquez[2]
[1]*Instituto Mexicano del Petróleo, Mexico City, Mexico*
[2]*Instituto de Geofísica Universidad Nacional Autónoma de México, Mexico City, Mexico*

Received: January 28, 2009; accepted: December, 2009

Resumen

Determinación de los límites locales de una columna estratigráfica (por ejemplo relacionados con ambientes de depósito) representan en particular una gran contribución al análisis y caracterización de yacimientos petroleros. En este marco general, las Transformadas de Ondícula, continua y discreta, son aplicadas a datos de registros geofísicos de pozos de un área productora de aceite en el Golfo de México, con el propósito de encontrar periodicidades o ciclos y correlacionarlos con las características litológicas y estratigráficas de los ambientes asociados.

Un análisis multiescala de registros geofísicos de pozos (rayos gama, resistividad y potencial espontáneo) fue realizado basado en la transformada de ondicular. En particular los coeficientes ondiculares fueron determinados. El análisis de los escalogramas-espectrogramas permitió obtener pseudolongitudes de onda características para cada escala (frecuencias). Las pseudolongitudes de onda fueron asociadas con posibles periodicidades o periodos deposicionales (ciclos climáticos de Milankovitch) del área de estudio.

El caso presentado muestra que el análisis ondicular es una técnica complementaria de gran ayuda para la caracterización de yacimientos, particularmente en la localización de secuencias estratigráficas y de las facies asociadas.

Palabras clave: Transformada de ondícula, registros geofísicos de pozos, patrones de repetición, análisis multiescala, ciclicidad.

Abstract

Establishment of sequence limits in a stratigraphic column (i.e., related to depositional environments) represents in particular a great contribution to the analysis and characterization of oil reservoirs. In this context, we applied the continuous as well as the discrete wavelet transforms, to data from geophysical well logs from an oil producing area in the Gulf of Mexico, in order to bring about periodicities or cycles and correlate them with lithologic and stratigraphic characteristics of the associated environments.

A multiscale analysis of geophysical well loggings (gamma ray, resistivity, and spontaneous potential) was done based in the wavelet transform. In particular the wavelet coefficients were determined. Analysis of the obtained spectrograms-scalograms enabled to establish characteristic pseudowavelengths for each scale (frequencies). Pseudo wavelengths were associated with possible periodicities in deposition (Milankovitch's climatic cycles) of the study area.

This case history shows that the wavelet analysis is a helpful complementary technique for reservoir characterization, specifically in the location of stratigraphic sequences and associated facies.

Key words: Wavelet transform, geophysical well logging, repetition patterns, multiscale analysis, cyclicity.

Introduction

The aim of static reservoir characterization is to produce models in particular of the spatial distribution of certain physical properties of rocks and of the contained fluids, constituting a given reservoir. The representative model is a product of multidisciplinary studies which are related to different types of geological and geophysical data (geological and structural aspects, geophysical well logs, core analysis, seismic data, hydrocarbon saturation, and pressure and production test information). A key factor in this context is the ciclicity of sedimentary formations.

The cycle stratigraphy (sequence stratigraphy) analyzes the cycles or periodicities to reconstruct and to define characteristic stratigraphic issues (Schwarzacher, 1998). Cycles are common in sedimentary environments, and they are represented by repetitive stratigraphic and depositional sequences. Two of the main causes of sedimentary cycles associated with changes in water level are tectonic movements and climatic changes.

It has been established the existence of sea level changes with five different types cycles with characteristic magnitude orders, with duration of about one hundred million to ten thousand years (Table 1) (Kerans and Tinker, 1997). Of these five cycle types, the fourth and fifth order cycles have durations of less than one million years and are considered as a regular cyclic control (Plint *et al*., 1993).

Changes in sea level, consequences of climatic effects, are identified as Milankovitch cycles. These are produced by three main aspects of the Earth's motion: rotation axis precession (21 x 10^3 years), obliquity variations of the rotating axis regarding the ecliptic (41 x 10^3 years) and eccentricity variations of the earth orbit (100 and 400 x 10^3 years).

Analysis of core and three-dimensional (3-D) seismic data analysis, as well as seismic interpretation play a definite role in the identification and correlation of stratigraphic units. Unfortunately, just a small percentage of the existing wells are cored.

In the same sense, it is known that seismic resolution associated with 3-D seismic data is not high enough to interpret stratigraphic sequences or facies location, because the vertical and horizontal seismic resolution depends both on the frequency and wavelength of the seismic information.

Therefore, other tools have been developed to help in the identification and correlation of stratigraphic units. Contrasting to the low number of wells being cored, geophysical well logs (GWL) are systematically obtained from most wells. Particularly, GWL categorically contribute to the geological evaluation and correlation (Coconi-Morales *et al*., 2005, 2006). GWL can register cyclicity, trends, sudden changes, etc. in sedimentation and stratigraphy.

The dip log (dipmeter) is one of the tools used to obtain predominant patterns, and assist stratigraphic correlation, identification of formation boundaries, and location of discordances, cyclicities or periodicities in the environments (Ramírez and Bueno, 1987; Doveton, 1994; Ramírez *et al*., 2000). Standard analysis tools applied in the determination of cyclicities or periodicities include: 1) semivariograms (SV) (Jennings *et al*., 2000; Jensen *et al*., 2000), 2) Fourier analysis (Gelhar, 1993), 3) and the biostratigraphic and chronostratigraphic methods and sequence stratigraphy (Prokoph and Agterberg, 2000).

Prokoph and Agterberg (2000) applied Morlet-wavelet based wavelet analysis to gamma-ray (GR) logs to localize discontinuities and to establish sedimentary cycles with high-resolution. They found a correlation between the predominant cycles within the GR logs with the relationships existing between the different Milankovitch cycles, suggesting that climatic cycles are an important factor in deposition.

The application of the GWL in sedimentary and stratigraphic studies has been intensified in recent decades (Serra and Abbot, 1982; Saggaf and Lebrija, 2000; Lee *et al*., 2002).

In particular, the wavelet based multiscale analysis of GWL has been developed (Prokoph and Agterberg, 2000; Bernasconi *et al*., 1999), and represents opportunities for research and technologic development, which, combined with structural and stratigraphic seismic interpretation, will contribute to the different stages of reservoir characterization.

In this study we apply Wavelet Transform (WT) to determine periodicities through pseudowavelengths. However, the proposed methodology differs from previous ones. Here first an analysis of the used wavelet is made (wavelet type) and then the length of the signal, sampling interval, and the scale range (minimum and maximum to be disturbed by means of the continuous wavelet transform -CWT, and by the discrete wavelet transform, DWT) are taken into account for a suitable correlation and determination of optimal scales. The

Table 1

Orders of cyclicity (Kerans and Tinker, 1997)

Cycle (order)	Stratigraphic Sequence	Duration (my)	Relative sea level (m)	Relative sea level rise/fall rates (cm/1000 yr)
First		> 100		<1
Second	Supersequence	10-100	50-100	1-3
Third	Depositional sequence	1-10	50-100	1-10
Fourth	High frequency sequence, parasequence	0.1-1	1-150	40-500
Fifth	High frequency cycle parasequence	0.01-0.1	1-50	60-700

pseudoperiodicities are estimated by the following sequence: i), determination of the number of scales to use in the CWT and in the DWT; ii) the scalogram and its coefficients are obtained; iii) the pseudo wavelength is obtained within the scalogram based on the scales and central frequency of the wavelet employed; and finally iv) a multiscale analysis is performed in the DWT domain for the detection of the layer limits.

Theoretical background of wavelet transform

Geophysical well logs (GWL) document different events and stratigraphic characteristics, e.g., cyclicity, trends, sudden changes, etc., which, as already mentioned have been traditionally studied by means of Fourier spectral synthesis and analysis. However Fourier analysis has a big limitation associated with time-space location. In the 1980's this limitation was partially overcome by the introduction of the WT. It represents a signal or image in different resolutions (multiscale) (Goswami and Chan, 1999).

The WT meaningfully contributes to the analysis and processing of geophysical data, and particularly with several potential applications to GWL.

In investigations related to geophysical signal analysis, the wavelet transform (Mallat, 1998) is, in general, an adequate technique for the preadjustment, analysis, and interpretation of signals and images on diverse representation scales (multiscale analysis) (Cohen and Chen, 1993; Li and Ulrych, 1995; Grubb and Walden, 1997; Lozada-Zumaeta and Ronquillo-Jarillo, 1997; Lozada-Zumaeta and Ronquillo-Jarillo, 2001; Matos *et al*., 2003; Gersztenkorn, 2005; Rivera-Recillas *et al*., 2005). The WT has been applied particularly in seismic data processing and pre-processing phase (Chakraborty and Okaya, 1995), in 1-D seismic inverse tomography problems (Xin-Gong and Ulrych, 1995), and in correlating and re-scaling petrophysical properties and seismic sections (Panda *et al*., 2000). In geosciences, in general is being applied to the analysis of transitory signals and image processing (Foufoula-Georgiou and Kumar, 1994), particularly in the detection of pseudo- periodicities in climatology (Lau and Weng, 1995).

Applications, in the oil industry, comprise the preadjustment, filtering, and anomaly identification of pressure tests (Jansen and Kelkar, 1997; Athichanagorn *et al*., 1999; Gonzalez *et al*., 1999; Soliman *et al*., 2001), compression-transmission of drilling data (logging while drilling) (Bernasconi *et al*., 1999).

A wavelet (mother wavelet) is defined by a located and oscillating function of time (Deighan and Watts, 1997; Burke, 1998). Examples of different types of wavelets are shown in Fig. 1 (Daubechies, 1990). The wavelet analysis synthesizes a nonstationary signal in terms of base functions (of time and frequency). From the mother wavelet $\psi_{(a,b)}$, the respective family wavelets are derived by means of scaling and translation procedures by manipulating the coefficients ***a*** (scale factor) and ***b*** (displacement or translation), respectively (Table 2).

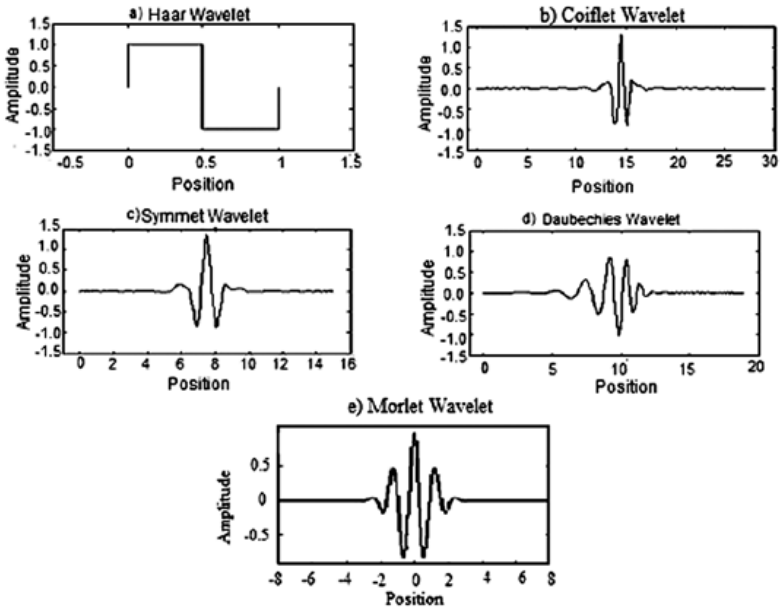

Fig. 1.- Wavelets types: a) Haar, b) Coiflet, c) Symmet, d) Daubechies and e) Morlet.

The coefficients distribution of a WT is presented in the time-frequency domain (Fig. 2). A summary of main wavelets types and their properties is given in Table 3. In this study Coiflet and Symlet wavelets were used.

Table 2

Basic Components used in the estimation of the WT.

Translation	Scale change	Translation and scale change
ψ (t - b)	$\frac{1}{\sqrt{a}}\psi(\frac{t}{a})$	$\frac{1}{\sqrt{a}}\psi\left(\begin{matrix} t-b \\ a \end{matrix}\right)$

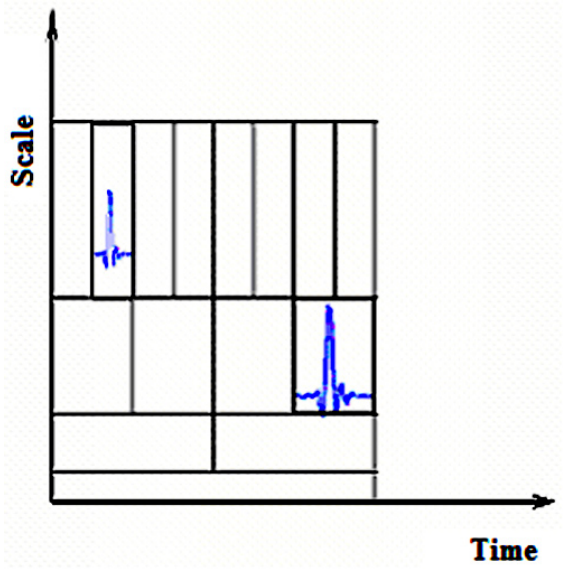

Fig. 2. Spectral density in the wavelet transform domain (time-frequency domain).

There are two types of wavelet transform, i.e., continuous and discrete.

(i) Continuous Wavelet Transform

The CWT (Grossman and Morlet, 1984) of a signal *x(t)* is defined as (Strang, 1989):

$$CWT(a,b) = \int_{-\infty}^{\infty} x(t)\, W_{ab}(t)dt = \frac{1}{\sqrt{|a|}}\int_{-\infty}^{\infty} x(t)\, \mathrm{W}\left(\frac{t-b}{a}\right)dt \quad (1)$$

where W is a function that is generated from the mother wavelet by translation and scaling; or in terms of spectral representation

$$CWT(a,b) = \sqrt{|a|}\int_{-\infty} x(\omega)\, W^{*}(a\omega)e^{ib\omega}\, d\omega \quad (2)$$

where * is the complex conjugate, ω frequency and $i = \sqrt{-1}$. The signal $x(t)$ must be of a finite energy. In this case, the signal $x(t)$ can be reconstructed or synthesized by means of the inverse continuous wavelet transform (ICWT) (Strang, 1989), defined as:

$$x(t) = C_g \iint CWT_x(a,b)\frac{1}{\sqrt{|a|}}W\left(\frac{t-b}{a}\right)\frac{dbda}{a^2} \quad (3)$$

C_g is a constant depending on the wavelet to be used (admissibility constant).

(ii) Discrete Wavelet Transform

In the discrete version of the WT, the parameters $\{(a_j, b_k)\}$ are respectively discretized, so that ψ_{a_j, b_k}, the wavelet family is defined as (Strang, 1989; Burke, 1998):

$$\psi_{a,b}(t) = \frac{1}{\sqrt{|a|}}\psi\left(\frac{t-b}{a}\right) \quad (4)$$

Table 3

Wavelet types and properties (Misiti *et al*., 1996; Daubechies, 1994).

Wavelet Type	Symlet	Morlet	Mexican Hat	Haar	Gaussian	Daubechies	Coiflet
Orthogonal	Yes	No	No	Yes	No	Yes	Yes
Biorthogonal	Yes	No	No	Yes	No	Yes	Yes
Compact support	Yes	No	No	Yes	No	Yes	Yes
DWT	Possible	No	No	Possible	No	Possible	Possible
CWT	Possible	Possible	Possible	Possible	Possible	Possible	Possible
Regularity				It is not continuous		About 0.2 N for large N	
Symmetry	Near	Yes	Yes	Yes	Yes	Far from	Near
Number of vanishing moments	N			1		N	2N

In general, these classes of wavelets are associated to a dyadic set (octave), $a_j = 2^{-j}$; $b_k = 2^{-j}k$ j, $k \in Z$, which transforms the expression (4) to the following one:

$$\psi_{jk}(t) = 2^{j/2}\left(2^j t - k\right) \quad j,k \in Z \tag{5}$$

and the DWT can occur as:

$$DW_\psi s(j,k) = \langle s, \psi_{j,k} \rangle = \int_{-\infty}^{\infty} s(t)\, \psi_{j,k}(t)\, dt \tag{6}$$

where $\psi_{j,k}(t)$ is the mother wavelet and $s(t)$ is a finite energy signal. On the other hand, the inverse transform (synthesis) is defined as:

$$s(t) = \sum_j \sum_k c_{j,k}\, \psi_{j,k}(t) \approx \sum_j \sum_k \langle s, \psi_{j,k} \rangle\, \psi_{j,k}(t) \tag{7}$$

$c_{j,k}$ are the appropriate wavelet coefficients.

Spectrogram and Scalogram

Spectrogram and scalogram are time-frequency graphical representations of the coefficients distribution associated with the WT, respectively, that may be related with energy and power spectra (Strang, 1989; Meyer and Ryan, 1993; Burke, 1998) of the $\psi(a, b)$,

$$\iint \psi(a,b)\, \frac{dbda}{a^2} \tag{8}$$

The energy distribution is associated to $\frac{\text{dadb}}{a^2}$.

The combination of the different coefficients at different scales (wavelengths) forms a scalogram. Depths versus coefficients indicate the position where the particular wavelength (λ) is placed. For the Coiflet wavelet, the scale to wavelength conversion is given by:

$$\lambda = \frac{1.25a}{Fs} \tag{9}$$

Where a is the scale and Fs is the sampling frequency. The wavelet analysis allows us to reveal aspects to small scales (high frequencies) and big scales (low frequencies).

Wavelet transform vs. semivariogram and Fourier transform

The semivariogram (SV) establishes the rate of similarity between a set of samples as a function of the separation, but the location of the cyclic events in the space is not possible neither as with the Fourier transform (FT). To illustrate this point we generated a series of synthetic signals, including a theoretical well log. We applied the conventional analysis techniques (SV and FT), as well as the WT, and conducted a comparative analysis.

In the first case, the FFT, SV, and WT (using a Morlet wavelet) were applied to a 1024 samples signal (sampling interval of 0.004 seconds, sampling frequency of 250 Hz, and a 125 Hz Nyquist frequency). The signal (Fig. 3a) comprises three components: a) a cosine function of 20 Hz frequency; b) an impulse located at 2 seconds; c) and a sweep from 2 to 15 Hz. Fig. 3b shows the FT of the resulting signal; the frequency components of the signals can be observed, but it is not possible to determine their time location.

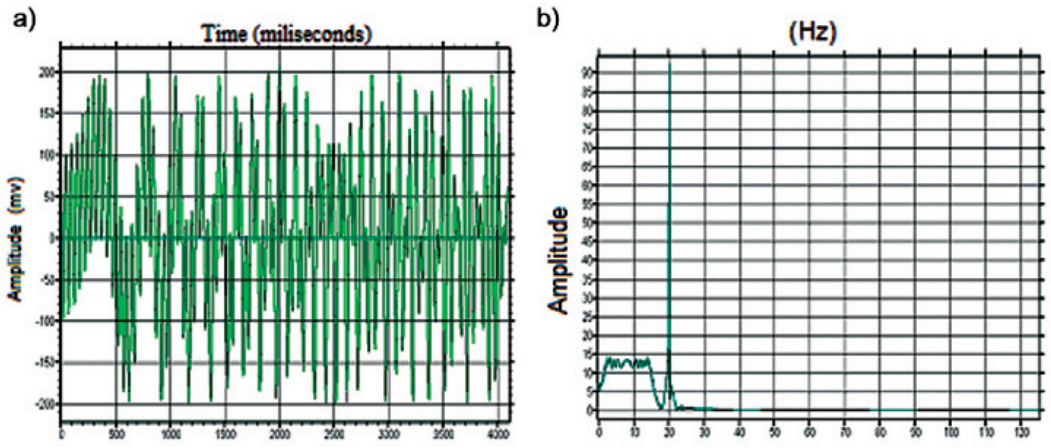

Fig. 3. a) Signal comprising a pulse, a cosine signal (20Hz), and an ascending signal (sweep) of 2 to 15 Hz. b) The amplitude spectrum of the resulting signal.

Fig. 4 displays the WT scalogram or coefficients distribution generated with the WT to the signal of Fig. 3a. The location (or domain) where the three component signals are active are very well represented. The characteristic frequency of the cosine signal, 20 Hz, can be read very well in the time axis. The instantaneous pulse, located at 2000 milliseconds, is parallel to the frequency axis. The sweep is transversely presented through the high and low scale domain.

Figs. 5 and 6 show the comparison of the WT with FT and SV for signals more representative of stratigraphic cycles. The corresponding signals contain multiple frequencies with different time distributions. These signals can fairly well be representative of a high energy sedimentary sequence. Fig. 5 shows the analysis of this signal with the three different methods (WT, FT and SV) applied to a two component signal. The first component, from 1000 to 1100 m, has an average wavelength of 33 m, while the second one, from 1100 to 1170 m, has an average wavelength of 13 m. The SV indicates fairly well the two components. The Fourier analysis shows more clearly than the semivariogram the presence of these two components; nevertheless these methodologies can display neither the location of the two components nor the frequency changes. In comparison, the scalogram (WT), identifies both frequencies accurately as well as the location of the corresponding transition.

The example of Fig. 6 again comprises two superimposed signals (with average wavelengths of 13 and 33 m respectively). Both, the SV and the Fourier analysis identify the presence of the two components, but are unable to locate them at depth. The scalogram besides identifying both signals helps to quantify the existing wavelengths. In particular it helps to identify the two overlapping existing cycles.

In both the above mentioned cases, SV and the Fourier analysis show similar results (two different wavelengths). However, the comparative analysis suggests that the analysis with the WT can provide better results, in relation with the Fourier analysis and the SV, in stratigraphic cycles studies. These results are in accordance with those reported by Lau and Weng (1995).

Finally, a pulsed neutrons (capture cross section or Sigma) synthetic log covering a depth interval of 0 to 4200 m, was generated (Fig. 7a). It is the theoretical response of a geological model comprising 24 thick and thin layers. For the generation of the synthetic sigma GWL, equation 10 was used (Dewan, 1983; Schlumberger, 1991; Coconi-Morales, 2000),

$$\Sigma_{\log}=S_w\phi\,(\Sigma_w-\Sigma_h)+\phi\,(\Sigma_h-\Sigma_{ma})+v_{sh}\,(\Sigma_{sh}-\Sigma_{ma})+\Sigma_{ma} \quad (10)$$

Where $\Sigma_{\log}$ is the capture cross section or sigma measured (in capture units, c.u.) for each depth; ϕ is porosity; S_w is water saturation (%); Σ_w and Σ_h are the sigma for water and oil (c.u.), respectively; v_{sh} is clay volume (%); Σ_{sh} is the sigma for clay (c.u.), and Σ_{ma} is the sigma of the associated matrix (c.u.).

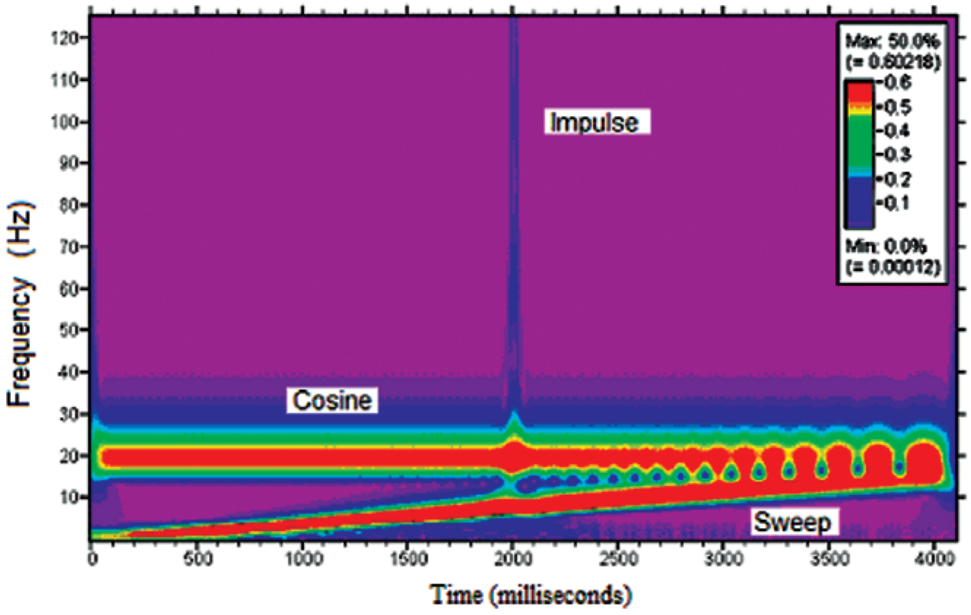

Fig. 4. Scalogram (wavelet coefficients distribution in the time-frequency space) of the signal presented in Fig. 3a.

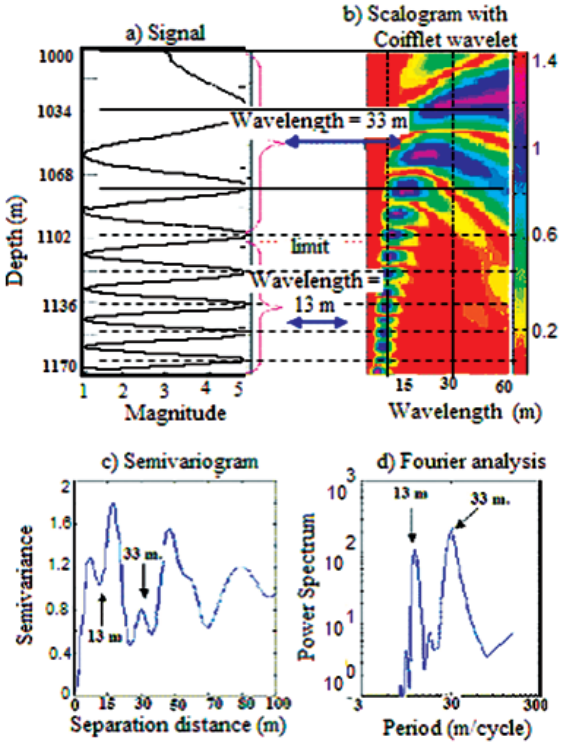

Fig. 5. Signal analysis for a continuous frequency change. a) Signal; b) Scalogram; c) Semivariogram and d) Fourier transform.

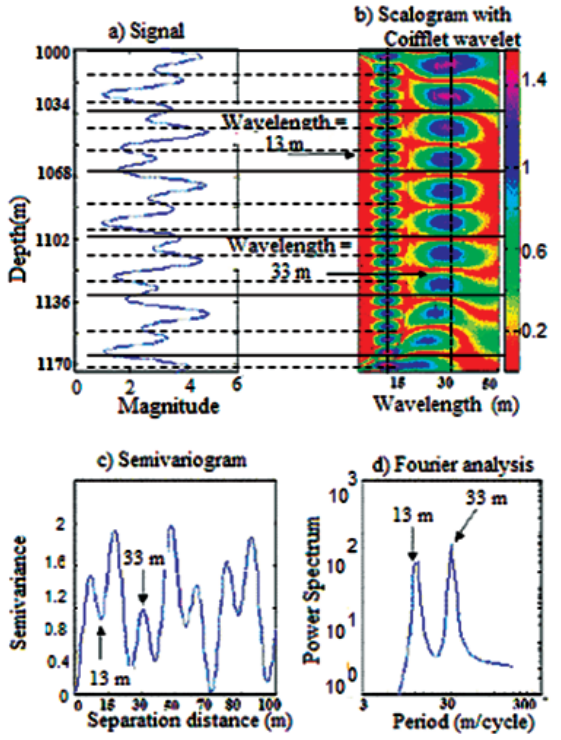

Fig. 6. Analyzed signal for two overlapping sedimentary cycles. a) Signal, b) Scalogram; c) Semivariogram, and d) Fourier transform

Sigma is the probability that gamma rays impact a nucleus thus rendering it possible to obtain water saturation, lithology and porosity of the formation under study.

The respective multiscale analysis is shown in Fig. 7b. It can be observed that for low scales (high frequencies) it is possible to distinguish thin layers, while at intermediate scales it is possible to analyze thicker layers. At even higher scales (low frequencies) the global characteristics are displayed. Thin layers would be represented as a single unit. For comparison purposes, the amplitude spectrum of the synthetic Sigma log is presented in Fig. 7c.

It is observed that the high frequencie spectrogram portion and corresponding to low scales (1, 2, 3 and 4), correlate with thin layers at depth intervals of 1200 – 1400, 2600 – 2800, and 4000 - 4200 m respectively (Fig. 7b).

Figs. 8 and 9 displays the representation of the theoretical log (Fig. 7a) at two different scales of the depth domain. From a set of different scale components, selectively chosen, it is possible to reconstruct, or synthesize, the theoretical log in such a way as to enhance predominant components at different frequencies. For example, scale 6 correlates with thin layers (Fig. 8). In Fig. 9 we can note how scale 9 enhances thick layers.

This comparative analysis also illustrates the methodology followed to determine cyclicity from the GWL, and which can be contrasted against the existing methods (i.e., that of Sadler, 1981). The methodology is schematized in Fig. 10.

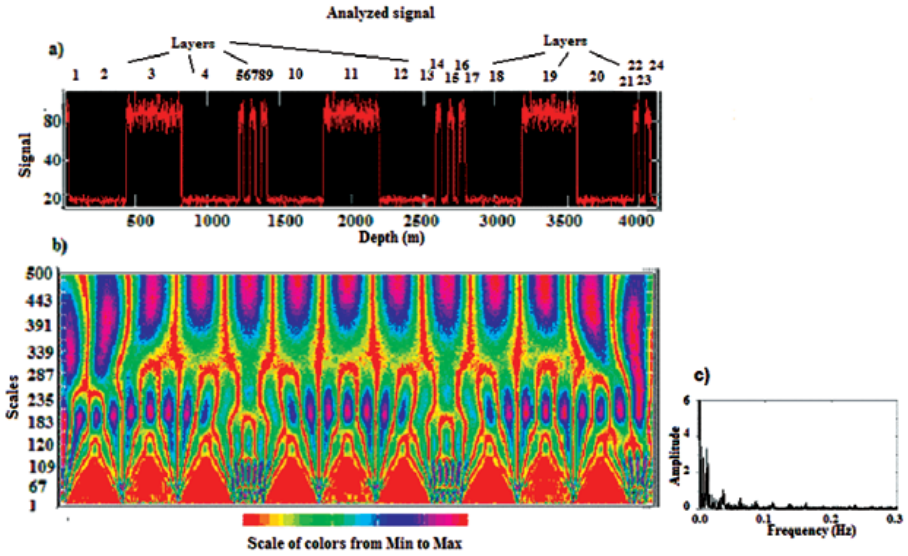

Fig. 7. CWT based multiscale analysis of a theoretical Sigma log. a) synthetic pulsated neutron (Sigma) log of a geological model constituted by 24 layers (thick and thin). b) the CWT. c) Amplitude spectrum.

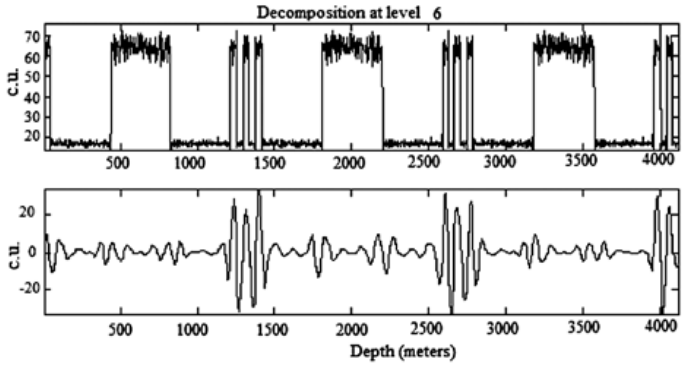

Fig. 8. Original signal (s), reconstruction using scale 6; thin layers are observed.

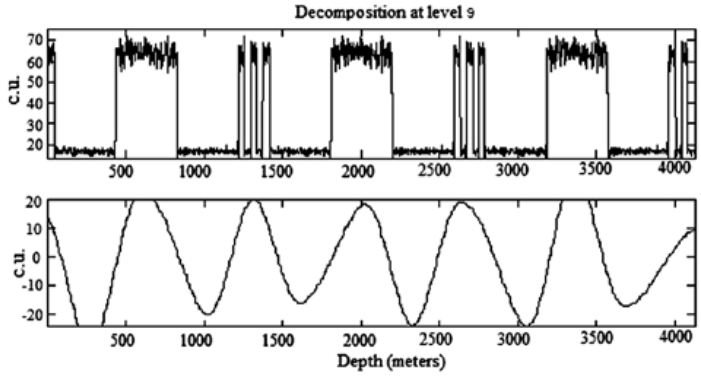

Fig. 9. Original signal (s) reconstruction using scale 9; thick layers are observed.

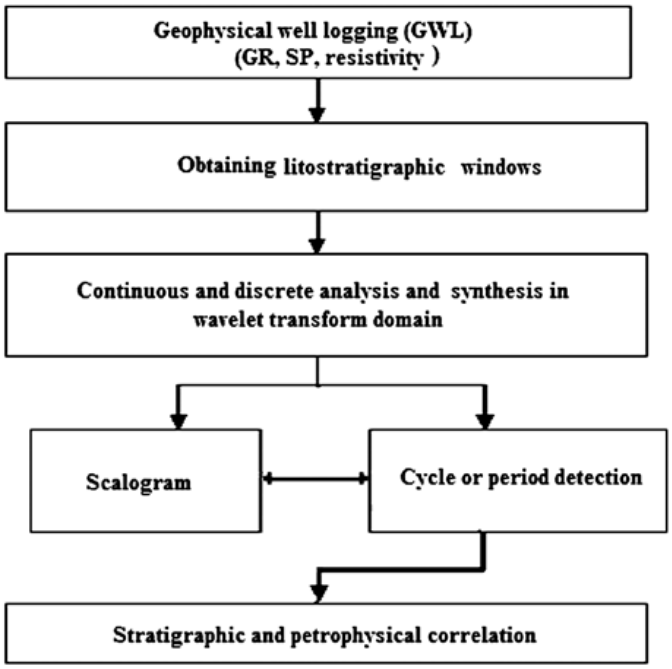

Fig. 10. Methodology for the analysis of cyclicities in GWL (SP, GR and Rt) with the CWT and the DWT.

The GWL lithoestratigraphic depth windows of interest (spontaneous potential -SP, GR, and true resistivity -Rt) are subjected to conventional analysis. Later the CWT is applied, involving two interrelated processes: the generation of the scalogram (selecting and using a specific wavelet), and the determination of cycles or discontinuities.

Application of the methodology

Multiscale analysis was applied to a set of GWL from a well of an area in the Gulf of Mexico. The representatives facies comprise sands, shales, and evaporites (Fig. 11c). The Coiflet wavelet (order 4, see Table 3) was selected to consequently obtain the CWT. Finally the characteristic pseudowavelengths linked to each of the representation scales were obtained from the corresponding scalogram.

Figs. 11a, b, e and g, represent respectively the permeability, natural GR, deep laterolog (LLD), neutron porosity (PHIN) and bulk density (RHOB) logs, in addition to the scalograms of the GR and Rt logs (Figs. 11d and 11f respectively). Stratigraphically, for its analysis, the well was divided in three main zones: zone 1 (1215 - 1250 m), zone 2 (1250 - 1275 2 m) and zone 3 (1275 – 1306 m).

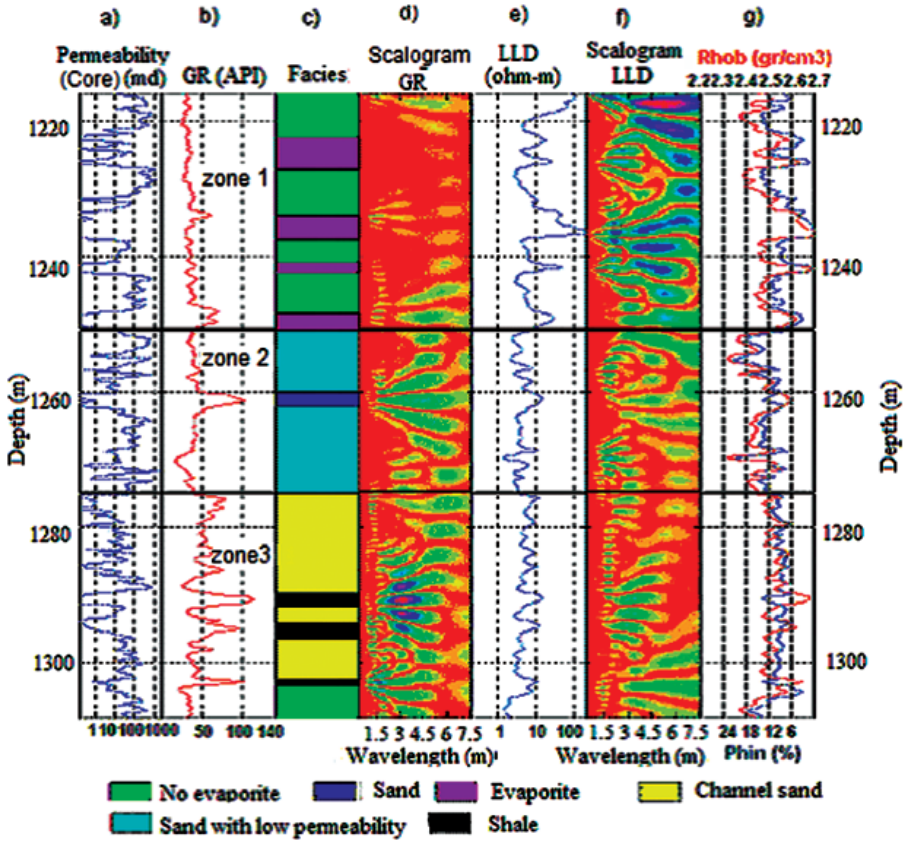

Fig. 11. Geophysical well log of the study area. a) core permeability, b) GR (API) log, c) sedimentary facies; d) WT scalograms using Coiflet wavelet (order 4) of the gamma-ray (GR), e) laterolog-deep log, (LLD) f). WT scalograms using Coiflet wavelet (order 4) of the laterolog-deep log, (LLD), g) Rhob (bulk density) and PHIN (neutron porosity).

Zone 1 comprises two evaporitic sequences (of low and high permeability) and an intermediate layer with no evaporites. The GR log only determines dirty zones (presence of shales) or clean zones (no shales) but not lithology type. The evaporite sequences are distinguished by means of the Rt log (LLD) (as resistivity increases), the neutron log (as low porosity values), and density log (as high values).

Accordingly, zone 1 shows cyclicities with periodicities ranging between 1.5 and 2 m, corresponding to the thickness of channelized or evaporatic deposits.

Additionally, the gamma ray scalogram shows short cycles for zone 1 with periods varying from 1.5 to 6 m. The LLD log shows strong cycles with periodicities varying respectively from 1.5 to 2.5 m, and 5 to 6 m.

Zone 2 comprises two zones, of high and low permeability sands respectively. Zone 3 is constituted by high permeability sands intercalated with low permeability clays.

Despite the mentioned limitations of the GR log, the respective scalogram displays or shows the limits of the thin anhydrite layers whose exact locations could be independently checked by means of core and petrophysical interpretation (Figs. 11a and c). Anomalies at different scales (frequencies) are observed in this scalogram. Low and intermediate scales correspond to the limits of thin and intermediate layers and sedimentary cycles, respectively.

For zones 2 and 3 a similar behavior is inferred due to the presence of clean sand layers. From the respective scalograms of the GR and LLD logs wavelengths were calculated ranging from 1 to 7.5 m. According to the GR log, zone 3 show cyclicities with periodicities ranging between 1.5 and 2 m.

Summarizing:

Zone 1: Displays a cyclicity of 1.5 to 2 m (cemented evaporites) at depth intervals of 1234 to 1236, 1239 to 1240, and 1248 to 1250 m. The GR log shows 1.5 and 6 m cyclicities, and the LLD log shows cycles ranging from 1.5 to 2.5, as well as from 5 to 6.5 m. Both scalograms solve layers thickness according to the depth information.

Zone 2: The GR log show a beach zone (sands), and together with the resistivity log (LLD), they enable to establish cycles with wavelengths between 1.5 to 2.5 m.

Zone 3: Cyclicities are comprised in the range of 1.5 to 2 m. The GR log registers cycles between 1 and 1.5 m (at the base) and of about 6 m (at the top). The GR log scalogram shows higher anomalies within the depth interval from 1290 to 1295 m, corresponding to zones containing clays. The GR log shows a progressive increase in radioactivity.

In zone 1, wavelengths are in the range from 1.5 to 2, and 3 to 7 m respectively, with a relationship from 1: 2: 4.6. For zone 2, the most characteristic –conspicuous wavelengths have values of 1 to 2, and 2.5 m as well as from 7 to 7.5 m with respective relationships of 1: 1.9: 4.8. Finally for zone 3, the three conspicuous wavelengths are of 1 to 2, 3, and 6.5 m, with corresponding relationship of 1: 2: 4.3.

Changes in sea level, consequences of climatic effects, are identified as Milankovitch's cycles. These are produced by three main aspects of the motion of the Earth rotation axis: precession ($21 \cdot 10^3$ years), obliquity variations of the rotating axis regarding the ecliptic ($41 \cdot 10^3$ years) and eccentricity variations of the earth orbit (100 and $400 \cdot 10^3$ years).

As already mentioned Milankovitch's cycles related to precession, obliquity of the rotation axis regarding the ecliptic, and eccentricity variations of the Earth orbit have respective periods of 21, 41 and 100 k years, with a respective relationship of 1: 2: 4.8.

A fair good correlation is observed between these relationship and those obtained for zone 2. This similarity in the relationships suggests that the Milankovitch's cycles played a key factor controlling the sand sedimentation in our study area.

To support this interpretation, one can calculate the sedimentation rate from the wavelet analysis, and compare it with information from previous studies. In particular, for a zone similar to our study area, during the Lower Triassic the sedimentation took place for 5 My. For the study area, the typical thickness of the corresponding formation is of 243 m; implying a sedimentation rate of 4.86 cm/kyear.

This result is within the range from 1.5 to 6 cm/kyear observed in sediments from this type and reported by Anstey and O'Doherty (2002). Based in the wavelet analysis, for zone 2, we observe that the dominant wavelength is 2.5 m (using the scale vs. energy graphs), (which corresponds to the Milankovitch's cycle related to obliquity of the rotation axis, with a period of 41 ky), and a sedimentation rate of 6.09 cm/kyear.

For zone 3, the dominate wavelength is of 1.1 m, that can be correlated with Milankovitch's cycle associated to precession of the rotation axis regarding the ecliptic, and with a period of 21 ky; we obtained a sedimentation rate of 5.24 cm/ky.

Conclusions

Wavelet analysis provides complementary information useful for the interpretation and evaluation of GWL. In particular, the wavelet based analysis when applied to information related to stratigraphic data can be a suitable technique in the study of stratigraphic cycles.

This study indicates: 1) that the SV and FT methods, the most commonly used methods so far, present limitations in the evaluation of overlapped cyclicities; and 2) that the wavelet transform and associated multiscale analysis are more suitable for establishment of cyclicities present in a sedimentary sequence.

A study case was presented that illustrates the potential of the wavelet analysis. It was possible, for a well from an area of Gulf of Mexico, to establish the cyclicity orders present in the intervals studied; which could be linked to the Milankovitch's cycles. The associated sedimentation rates correlate fairly well with independent information.

Acknowledgments

The authors greatly appreciate the support of the Instituto Mexicano del Petróleo for the development of the present study. Comments and suggestions of three anonymous reviewers helped to improve the quality of the paper.

Bibliography

Anstey, N. and R. O'Doherty, 2002. Cycles, layer and reflections: Part I: *The Leading Edge*, January, 21, 1, 44-51.

Athichanagorn, S., R. Horne and J. Kikani, 1999. Processing and interpretation of long-term data from permanent down hole pressure gauges, paper SPE 56419, in SPE Annual Technical Conference and Exhibition, Houston, October, 3-6.

Bernasconi, G., V. Rampa, F. Abramo and L. Bertelli, 1999. Compression of down hole data, paper SPE/IADC in SPE (IADC Drilling Conference), Amsterdam, 9-11 March.

Burke, H. B., 1998. The World according to wavelets. A. K. Peters (editor), second edition, 250 p.

Chakraborty, A. and D. Okaya, 1995. Frequency-time decomposition of seismic data using wavelet-based methods. *Geophysics, 60*, 1906-1916.

Coconi-Morales, E., 2000. Metodología usando el registro de neutrones pulsados (PNC) para el monitoreo de los contactos gas – aceite y aceite – agua y saturación de agua en el complejo Cantarell. Master's degree thesis, División de Estudios de Posgrado, Facultad de Ingeniería, Universidad Nacional Autónoma de México, 100 p.

Coconi-Morales E., M, Lozada-Zumaeta, D. Rivera-Recillas and G. Ronquillo-Jarillo, 2005. Estimación litoló-gica a partir de registros geofísicos de pozo utilizando trasformada de ondícula discreta unidimensional (DWT 1-D). First Geosciences Internacional Con-gress, September 4-7, Mérida, Yucatán, México, p. 130 – 135.

Coconi-Morales, E., M. Lozada-Zumaeta, D. Rivera-Recillas, G. Ronquillo-Jarillo and J. O. Campos-Enriquez, 2006. Identifying reservoir fluids in sandy clay and carbonate reservoir using the wavelet transform with well logs. SPWLA 47th Annual Logging Symposium, June 4-7, Veracruz, Mexico, p. 130-135.

Cohen, J. and T. Chen, 1993. Fundamental of the wavelet transform for seismic data processing. Tech Rep. CWP-130. Center for wave phenomena. CSM, 250 p.

Daubechies, I., 1990. The wavelet transform, time-frequency location and signal analysis, IEEE Transactions on Information Theory, 36, 5.

Daubechies I., 1994. Ten lectures on wavelets, CBMS, SIAM, 258-261.

Deighan, A. and D. Watts, 1997. Ground roll suppression using the wavelet transform. *Geophysics, 62*, 1896-1903.

Dewan, J., 1983. Modern open-hole log interpretation. Pennwell Books. 361p.

Doveton, J., 1994. Geologic log analysis using computer methods, AAPG Computer Applications in Geology, 2, Tulsa. 162 p.

Foufoula-Georgiou, E. and F. Kumar, 1994. Wavelet in Geophysics Academic Press, New York, p. 1-43.

Gelhar, L., 1993. Stochastic subsurface hydrology, Prentice-Hall, Englewood Cliffs, N.J., 250 p.

Gersztenkorn, A., 2005. Stratigraphic detail from wavelet based spectral imaging. CSEG Record. April, p. 40-43.

Gonzalez, F., R. Camacho and B. Escalante, 1999. Truncation de-noising in transient pressure test, paper SPE 56422, in SPE Annual Technical Conference and Exhibition, Houston, October 3-6, 234-239.

Goswami, J. and A. Chan, 1999. Fundamentals of wavelet, John Wiley, New York, 324 p.

Grossman, A. and J. Morlet, 1984. Descomposition of hardy functions into square integrable wavelets of constante shape. *SIAM J. Math. Annal., 15, 4*, 723 p.

Grubb, H. and A. Walden, 1997. Characterizing seismic time series using the discrete wavelet transform. *Geophysical Prospecting, 45*, 183-205.

Jansen, F. and M. Kelkar, 1997. Application of wavelet to production data in describing inter-well relationships, paper SPE 38876, in Annual technical conference and exhibition: Society of Petroleum Engineers, 323-330.

Jennings, J. W., S. C. Ruppel and W. B. Ward, 2000. Geostatical analysis of permeability data and modeling of fluid-flow effects in carbonate outcrops: SPEREE, 3, 292-303.

Jensen, J. L., L. Lake, P. Corbett and D. Goggin, 2000. Statistics for petroleum engineers and geoscientist. Elsevier, Amsterdam, 364 p.

Kerans, Ch. and Tinker S., 1997. Sequence stratigraphy and characterization of carbonate reservoirs. SEPM. Short course notes 40, 1-38.

Lau, K. and H. Weng, 1995. Climate signal detection using wavelet transform: How to make a time series, *Bull. of the Am. Meteorological Society. 76,* 12, p. 2391-2402.

Lee, S. H., A. Khargonia and A. Datta-Gupta, 2002. Electrofacies characterization and permeability predictions in complex reservoirs. *SPE Reservoir Evaluation & Engineering, 5*, 3, 237-248.

Li, X. and T. Ulrych, 1995. Tomography via wavelet transform constraints. 65th Annual International Meeting, Society Exploration Geophysicists, Expanded Abstracts, 1070–1073.

Lozada-Zumaeta, M. and G. Ronquillo-Jarillo, 1997. Multiresolution Analysis and Seismic Attributes. Moscow International Geoscience Conference, Exhibition. Soc. E.G.S, EAGE and SEG. Expanded Abstracts, 245-250.

Lozada-Zumaeta, M. and G. Ronquillo-Jarillo, 2001. Transformada de ondícula aplicada al análisis sísmico de reflexión. Séptimo Congreso Internacional SGGF. 493-496. Salvador, Brasil.

Mallat, S., 1998. A wavelet tour of signal processing. Academic Press, New York, 140 p.

Matos, C., P. Osorio and P. Johann, 2003. Using wavelet transform and self organizing maps for seismic reservoir characterization of a deep water field, Campos Basin, Brazil. SEG Expanded Abstracts, P. 120-124.

Meyer, Y. and R. Ryan, 1993. Wavelet Theory & Applications, Cambridge University Press, 528 p.

Misiti, M., Y. Misisit, G. Oppenheim and J. Poggi, 1996. Wavelet Toolbox. The Math Works, Inc. New York. 320 p.

Panda, M. N., C. C. Mosher and A. K. Chopra, 2000. Application of wavelet transform to reservoir-data analysis and scaling. SPE, 5, 92-101.

Plint, A. G, N. Eyles and R. G. Walker, 1993. Control of sea leavel change. Geological Association of Canada, Toronto, 15-25.

Prokoph, A. and F. G. Agterberg, 2000. Wavelet analysis of well-logging data from oil source rock, Egret member, offshore eastern Canada. *AAPG Bull. 84, 10*, 1617-1632.

Ramírez, J. H. and O. Bueno, 1987. Correlación de Registros Utilizando Técnicas de Inteligencia Artificial, Rev. AIPM, Vol. XXVII., 45-50.

Ramírez, J., Morfín-Faure M. and E. Coconi-Morales, 2000. Manual de capacitación en registros geofísicos de pozo, Instituto Mexicano del Petróleo, 80 p.

Rivera-Recillas, D., M. Lozada-Zumaeta, Ronquillo-Jarrillo and J. O. Campos-Enríquez, 2005. Multiresolution analysis applied to interpretation of seismic reflection data. *Geofísica Internacional. 44,* 355 – 368.

Sadler, P., 1981. Sediment accumulation rates and the completeness of stratigraphic sections. *Journal of Geology. 89,* 569-584.

Saggaf, M. M., and E. L. Lebrija, 2000. Estimation of lithologies and depositional facies from wire-lines longs. *AAPG Bull. 84,* 1633-1646.

Schlumberger, 1991. Dual-burst TDT logging. Texas, 33 p.

Schwarzacher, W., 1998. Stratigraphic resolution, cycles and sequences. Sequence stratigraphy. Concepts and applications. Elsevier, Amsterdam, 243 p.

Serra, O. and H. T. Abbot, 1982. The contribution of logging data to sedimentology and stratigraphy. *Society Petroleum Engineers Journal. 22,* 117-135.

Soliman, M. Y., J. Ansah, S. Stephenson and B. Manda, 2001. Application of wavelet transform to analysis of pressure transient data. Paper SPE 71571, in: SPE Annual Technical Conference and Exhibition. New Orleans, 30 Sept-3 Oct., 1234-1238.

Strang, G., 1989. Wavelets and dilation equations: A brief introduction, SIAM review, 31, 614-627.

Xin-Gong, L. and T. J. Ulrych, 1995. Tomography via wavelet transform constrain, University of British Columbia. 65th ann. International Meeting. Society of Exploration Geophysicists. Expanded abstracts, 1070-1073.

E. Coconi-Morales[1*], G. Ronquillo-Jarillo[1], O. Campos-Enríquez[2]

[1]Instituto Mexicano del Petróleo, Eje Central Norte Lázaro Cárdenas 152, 07730, Mexico City, Mexico

[2]Instituto de Geofísica, Universidad Nacional Autónoma de México, Ciudad Universitaria, Del. Coyoacán, 04510, Mexico City, Mexico

**Corresponding author: ecoconi@imp.mx*